Published in final edited form as:
Curr Opin Neurobiol. 2007 October ; 17(5): 593–600. doi:10.1016/j.conb.2007.11.002.

MRI Contrast Agents for Functional Molecular Imaging of Brain Activity

Alan Jasanoff[1,*]

[1] Departments of Nuclear Science & Engineering, Biological Engineering, and Brain and Cognitive Sciences Massachusetts Institute of Technology 150 Albany St., NW14−2213 Cambridge, MA 02139

Summary

Functional imaging with MRI contrast agents is an emerging experimental approach that can combine the specificity of cellular neural recording techniques with noninvasive whole-brain coverage. A variety of contrast agents sensitive to aspects of brain activity have recently been introduced. These include new probes for calcium and other metal ions that offer high sensitivity and membrane permeability, as well as imaging agents for high resolution pH and metabolic mapping in living animals. Genetically-encoded MRI contrast agents have also been described. Several of the new probes have been validated in the brain; *in vivo* use of other agents remains a challenge. This review outlines advantages and disadvantages of specific molecular imaging approaches and discusses current or potential applications in neurobiology.

Keywords

fMRI; hemodynamics; calcium; pH; metabolism; genetic

Introduction

As neuroscientists become increasingly brave in their efforts to study the functioning of neural systems *in vivo*, there is a growing need for measurement methods that can record comprehensive information about the functioning of living brains. Magnetic resonance imaging (MRI) is a special tool in this regard, because of its relatively high spatial resolution (~ 10 μm in high magnetic field scanners) and capacity to scan entire organisms noninvasively. Functional MRI (fMRI) with contrast dependent on cerebral hemo-dynamics provides an indirect readout of neural activity [1-3]. Although hemodynamic fMRI has had transformative impact in cognitive science, the techniques lack the specificity and temporal precision of electrophysiology and optical imaging, and have not been widely used in basic neurobiology experiments.

Another way to exploit the unique advantages of MRI for neuroscience is to perform the imaging in conjunction with molecular probes (contrast agents) sensitive to aspects of neuronal physiology [4]. This approach is roughly analogous to performing optical neuroimaging with

* Address correspondence to AJ *tel.:* 617−452−2538 *fax:* 617−253−0760 *e-mail:* jasanoff@mit.edu.

fluorescent dyes, but is currently far less well-developed. Most MRI contrast agents are paramagnetic chemicals that increase parameters called the T_1 and T_2 relaxation rates of water, as observed in tissue and solution; T_1 or T_2 relaxation enhancements produce image brightening or darkening, respectively. Additional classes of contrast agents work by a chemical exchange-based mechanism called CEST [5], or involve imaging nonstandard nuclei like ^{19}F and ^{13}C. The characteristics and physical mechanisms of different types of contrast agent are discussed at length in a number of book chapters and reviews [6-11], and are summarized in Figure 1. In general, for any agent to be used in functional imaging, either its ability to influence MRI contrast or its spatial distribution must be sensitized to neural activity in some way.

The past few years have seen significant advances in the design of new MRI contrast-based sensors and the introduction of protein contrast agents for brain imaging. These are nascent technologies—few of the efforts have progressed beyond an *in vitro* or proof-of-concept stage, but in several cases experiments using the new agents in animals can now be performed. The remainder of this review describes contrast agents suitable for functional imaging based on metal ions, pH, metabolic activity, and gene and protein expression. Prospects for future development and application of molecular fMRI methods are discussed.

Indicators for Ca^{2+} and other metal ions

Calcium ions are an important target for neuroimaging agents because neuronal calcium fluxes are dramatic and directly related to synaptic activity. Recent two-photon fluorescence imaging studies have demonstrated the power of calcium measurements to characterize neuronal population behavior in exposed regions of the brain [12,13]. MRI indicators for calcium can facilitate calcium imaging of deep tissue structures. Several relaxation-based contrast agents for calcium-dependent MRI have been introduced. An increasingly widespread approach was introduced by Koretsky and colleagues, who showed that Mn^{2+} functions as a paramagnetic Ca^{2+} mimetic and accumulates activity-dependently in neurons [14,15]. Because of its slow uptake and release kinetics (on the order of hours and days, respectively [16]), Mn^{2+} has proved useful as an “activity label” analogous to 2-deoxyglucose or c-Fos. The technique was recently used for 100 μm isotropic resolution T_1-weighted mapping of auditory cortex in mice [17], and for a functional study of the antennal lobes of developing moths [18].

A contrast agent sensor designed for real-time calcium imaging was developed by Li *et al.* [19]. The agent was formed by attaching the calcium chelator 1,2-bis-(O-aminophenoxy) ethane-N,N,N',N'-tetraacetic acid (BAPTA) to two copies of the highly paramagnetic gadolinium complex Gd^{3+}-1,4,7,10-tetraazacyclododecane-1,4,7,10-tetraacetic acid (Gd-DOTA); the agent undergoes a change in T_1 relaxivity (a measure of efficacy) near 1 μM Ca^{2+}. Delivery of the sensor to neurons in sufficient quantity for functional imaging *in vivo* has not yet been reported. Partly in response to this situation, Atanasijevic *et al.* [20] have now described a new family of calcium sensors derived from extremely potent superparamagnetic iron oxide (SPIO) nanoparticle contrast agents. SPIOs were conjugated to “tunable” recombinant proteins that drove reversible particle aggregation around a midpoint of 0.8 μM Ca^{2+} and produced over 100% T_2-weighted MRI signal changes *in vitro*. A key advantage of the these agents is that because of their high relaxivity, they may be used at concentrations (~ 1 nM) that are both easier to deliver and less disruptive to cellular calcium dynamics than Gd^{3+}-based sensors (effective at 10−100 μM). A disadvantage of the SPIO calcium sensors is that they respond relatively slowly to calcium changes [21]. As with the Gd^{3+}-based calcium sensors, fMRI with SPIO sensors could be possible once effective intracellular delivery strategies are harnessed; SPIO uptake by brain cells *in vivo* has been demonstrated [22,23].

Ions of transition metals such as zinc and copper are also influenced by neural activity, and alterations of transition metal homeostasis have been associated with a number of neuropathologies. Gadolinium-based sensors for zinc [24] and copper [25], similar to the Li

et al. [19] calcium sensor, have been synthesized and shown to produce T_1 relaxation changes *in vitro*. Zhang *et al.* [26] recently introduced an MRI zinc sensor derived from the Mn^{3+} complex with 5,10,15,20-tetraphenylporphinetetrasulfonic acid (Mn-TPPS). Because their porphyrin framework and zinc-binding moieties are amphiphilic, these contrast agents are cell permeable. The authors demonstrated zinc-dependent MRI signal changes in cells incubated with the agent. Future studies will indicate to what extent this approach can be applied in intact animals.

pH indicators

The extracellular medium becomes slightly acidified during neural activity [27]. Although these changes (in the range from pH 7.2−7.4) are not restricted to individual neurons, they could be monitored by pH-sensitive probes and used for functional fMRI. Both relaxation and CEST-based MRI contrast agents work by mechanisms that involve water or proton exchange (Figure 1A-C), which are inherently pH dependent and therefore easily compatible with pH sensing. In fact, a diverse set of pH indicators for MRI has been described (reviewed in [28]), though none of the indicators has yet been demonstrated to detect changes in neuronal activity. In one of relatively few *in vivo* studies, Garcia-Martin *et al.* [29] used a phosphonated Gd^{3+}-based contrast agent to measure intravascular acidification in rat gliomas. Differences of the order of one pH unit could be distinguished, and absolute pH values were obtained using a calibration procedure [30]. The contrast agent used in this study experiences changes in T_1 relaxivity over the broad range from pH 6−8 [31]; the sensor could in principle be applied for functional brain imaging, following intracranial injection or blood-brain barrier disruption, but MRI signal changes would be expected to be less than one percent under realistic pH fluctuations (< 0.2 units) and agent concentrations (~ 100 μM). Synthesis of novel sensors optimized for sensitivity in the pH 7.2−7.4 range may therefore be critical to developing this approach for fMRI. An alternative is the use of intrinsic protein amide proton contrast for CEST-related pH imaging in the brain [32]. Initial studies applied this method to detect focal ischemia in rats, involving pH changes on the order of 0.5 units.

Probes for metabolic activity

Changes in metabolic activity are closely coupled to neural signaling, and MRI contrast agents sensitive to cellular respiration may be used for functional imaging. Given evidence that metabolic processes including the consumption of oxygen are locally regulated on a much faster timescale than changes in hemodynamics [33], direct monitoring of these variables could provide more precise information about brain function than hemodynamic fMRI techniques can. The best known oxygen sensitive contrast agent is the endogenous iron containing protein hemoglobin, which underlies blood oxygen level dependent (BOLD) contrast [34]. Hemoglobin can also be used as an exogenous sensor in tissue [35], but it does not seem to provide enough sensitivity to detect rapid deoxygenation events (“initial dips”) associated with changes in neural activity. Cerebral metabolite uptake has traditionally been measured using radioactive glucose analogs, in conjunction with positron emission tomography (PET) or postmortem autoradiography. Golman *et al.* [36] have now introduced a sophisticated technique for performing similar experiments by MRI. The technique involves following the kinetics of a ^{13}C-labeled metabolite, pyruvate, by ^{13}C MRI (Figure 1D). Normally, ^{13}C MRI is too insensitive to detect pyruvate at physiologically relevant concentrations, but here the authors used a method called dynamic nuclear polarization to boost the MRI signal from $^{13}C_1$-pyruvate using a specialized device [37]. Kinetics of pyruvate uptake and turnover to lactate and alanine were followed in the muscles and abdominal organs of rats and pigs. Whether this or related approaches can be useful for functional brain imaging is unclear at present. Principal difficulties involve the relatively rapid decay of MRI signal from the tracer (time constant 15−20 s *in vivo*), the fact that other metabolites (*e.g.* glucose) have much shorter

decay times, and the need in fMRI applications for periodic or continuous supply [38] of polarized agents to the brain.

Genetically-controlled contrast agents

The discovery of green fluorescent protein (GFP) and the development of genetically-encoded fluorescent indicators like cameleons [39] and synaptophluorins [40] are continuing to revolutionize the modern practice of neuroscience. Unlike fluorescent proteins, genetically encodable contrast agents (most of them paramagnetic metalloproteins) are plentiful in nature, but it is only in the past few years that any of these have been exploited as ectopically expressed markers for imaging. The iron storage protein ferritin (Ft) encloses a core of ferrihydrite with partially superparmagnetic properties, making Ft a close natural analog of SPIO contrast agents [41]. In a 2005 paper, Genove *et al.* [42] demonstrated that viral-mediated overexpression of Ft in mouse brain led to clear changes in T_2-weighted images (Figure 2A). Iron loading and relaxivity changes induced by Ft can be boosted by co-expressing transferrin receptor, another participant in endogenous iron metabolism [43]. A recent report has now shown that Ft subunits expressed in transgenic mice can be detected in multiple tissue types and *in utero* without pathological side-effects [44], suggesting that Ft may find broad utility as a marker protein in MRI. This study showed that Ft expression even in relatively sparse endothelial cells led to detectable contrast changes (Figure 2B). Another protein contrast agent was cleverly designed by Gilad *et al.* [45], who boosted the concentration of exchangeable amine protons in transfected cells using an artificial lysine rich protein (LRP). Using the CEST MRI method (see Figure 1C), cells expressing the LRP could be distinguished from controls both in test tubes and in xenografted tumors (Figure 2C). Unlike Ft, which requires iron loading to induce contrast, LRP is a contrast agent as soon as it is translated; this may permit LRP expression changes to be detected on a shorter timescale than changes in Ft levels. On the other hand, MRI signal changes reported by Gilad *et al.* [45] were relatively subtle and required long imaging times to resolve (> 30 min.), and it is not yet known whether LRP expression-mediated contrast may be generalized easily to other contexts.

How could genetically encoded contrast agents be used for functional brain imaging? Although this has not been reported, a technically straightforward approach would be to express a protein contrast agent under control of a promoter known to be regulated by neural activity, like those of immediate early genes (IEGs) *fos* and *arc*. Because IEG protein induction generally persists for hours [46], a method like this would not be useful for functional imaging on the timescale of conventional fMRI or neurophysiology techniques, but it could be used in fairly simple (and potentially longitudinal) mapping studies in animals, somewhat like Mn^{2+} labeling technique discussed above. A more exciting direction from the perspective of systems neuroscience would be the engineering of MRI sensors for neural activity using protein contrast agents as building blocks. Key advantages of genetically encoded sensors over synthetic sensors include the possibility that they might be genetically targeted to specific cell types, the relative ease of delivering genes *vs.* imaging agents, and the fact that protein contrast agents may be cheaper to use and easier to modify than many synthetic contrast agents.

Genetic mechanisms can be used to direct MRI contrast due to exogenous agents; “semi-genetic” approaches to functional imaging might offer better sensitivity than protein contrast agent expression, particularly if high relaxivity agents or enzymatic amplification strategies are incorporated. Initial examples included detection of *lacZ* marker expression in developing frog embryos using a gadolinium-chelating β-galactosidase substrate [47], and monitoring of a transferrin receptor reporter gene in mice using transferrin-conjugated SPIOs [48]. Semi-genetic contrast mechanisms based on a variety of marker proteins and receptors have now been reported (reviewed in [49-51]), and design of contrast agents targeting RNA transcripts

has also been described [52,53]. Measurement of biological processes in the nervous system has not yet been convincingly demonstrated, however.

Conclusions

A number MRI contrast agents with potential utility for functional imaging have been discussed. Table 1 summarizes advantages and disadvantages of many of the approaches. Although some of the contrast agents have been applied in animals, only Mn^{2+} dependent labeling has so far been used for functional imaging of neural activity. For basic neuroscience studies, none of the new techniques is currently a surrogate for hemodynamic fMRI or invasive neural recording methods. Major progress has been achieved recently, however, with the development of new MRI probes for sensitive detection of brain-related physiological variables and the introduction of protein and genetically-controlled contrast agents. Several of these agents have been used to make measurements *in vivo*; applications to functional neuroimaging appear feasible in some cases, perhaps within the next five years. In addition to the persistent challenges of obtaining sensitivity and specificity for neural events, a hurdle in developing molecular fMRI techniques further will be the need to distinguish molecular signatures of activity from hemodynamic responses. Validation experiments in reduced preparations and in animals with suppressed BOLD responses may be valuable. Future work in this area will certainly focus on extending applications of the existing contrast agents in live animals, the development of more genetically-controlled probes, and the creation of MRI sensors for previously unexplored aspects of neural signaling, such as membrane potential and neurotransmitter release.

Acknowledgments

The author wishes to acknowledge support from the NIH (EB5723), the McKnight Endowment Fund for Neuroscience, and the Raymond and Beverly Sackler Foundation.

Abbreviations

BOLD	Blood Oxygenation Level Dependent
BAPTA	1,2-bis-(O-aminophenoxy)ethane-N,N,N',N'-tetraacetic acid
CaM	Calmodulin
CEST	Chemical Exchange Saturation Transfer
DNP	Dynamic Nuclear Polarization
DOTA	1,4,7,10-tetraazacyclododecane-1,4,7,10-tetraacetic acid
fMRI	Functional Magnetic Resonance Imaging
IEG	immediate early gene
SPIO	Superparamagnetic Iron Oxide
TPPS	5,10,15,20-tetraphenylporphinetetrasulfonic acid

References

1. Belliveau JW, Kennedy DN Jr. McKinstry RC, Buchbinder BR, Weisskoff RM, Cohen MS, Vevea JM, Brady TJ, Rosen BR. Functional mapping of the human visual cortex by magnetic resonance imaging. Science 1991;254:716–719. [PubMed: 1948051]
2. Kwong KK, Belliveau JW, Chesler DA, Goldberg IE, Weisskoff RM, Poncelet BP, Kennedy DN, Hoppel BE, Cohen MS, Turner R, et al. Dynamic magnetic resonance imaging of human brain activity

during primary sensory stimulation. Proc Natl Acad Sci U S A 1992;89:5675–5679. [PubMed: 1608978]

3. Ogawa S, Tank DW, Menon R, Ellermann JM, Kim SG, Merkle H, Ugurbil K. Intrinsic signal changes accompanying sensory stimulation: functional brain mapping with magnetic resonance imaging. Proc Natl Acad Sci USA 1992;89:5951–5955. [PubMed: 1631079]
4. Jasanoff A. Functional MRI using molecular imaging agents. Trends Neurosci 2005;28:120–126. [PubMed: 15749164]
5. Ward KM, Aletras AH, Balaban RS. A new class of contrast agents for MRI based on proton chemical exchange dependent saturation transfer (CEST). J Magn Reson 2000;143:79–87. [PubMed: 10698648]
6. Muller, RN.; Roch, A.; Colet, J-M.; Ouakssim, A.; Gillis, P. Particulate Magnetic Contrast Agents.. In: Merbach, AE.; Toth, E., editors. The Chemistry of Contrast Agents in Medical Magnetic Resonance Imaging. John Wiley & Sons; 2001.
7. Toth, E.; Helm, L.; Merbach, AE. Relaxivity of Gadolinium(III) Complexes: Theory and Mechanism.. In: Merbach, AE.; Toth, E., editors. The Chemistry of Contrast Agents in Medical Magnetic Resonance Imaging. John Wiley & Sons; 2001.
8. Allen MJ, Meade TJ. Magnetic resonance contrast agents for medical and molecular imaging. Met Ions Biol Syst 2004;42:1–38. [PubMed: 15206098]
9. Zhou J, Wilson DA, Sun PZ, Klaus JA, Van Zijl PC. Quantitative description of proton exchange processes between water and endogenous and exogenous agents for WEX, CEST, and APT experiments. Magn Reson Med 2004;51:945–952. [PubMed: 15122676]
10. Mansson S, Johansson E, Magnusson P, Chai CM, Hansson G, Petersson JS, Stahlberg F, Golman K. ^{13}C imaging-a new diagnostic platform. Eur Radiol. 2005
11. Yu JX, Kodibagkar VD, Cui W, Mason RP. ^{19}F: a versatile reporter for non-invasive physiology and pharmacology using magnetic resonance. Curr Med Chem 2005;12:819–848. [PubMed: 15853714]
12. Stosiek C, Garaschuk O, Holthoff K, Konnerth A. In vivo two-photon calcium imaging of neuronal networks. Proc Natl Acad Sci U S A 2003;100:7319–7324. [PubMed: 12777621]
13. Ohki K, Chung S, Ch'ng YH, Kara P, Reid RC. Functional imaging with cellular resolution reveals precise micro-architecture in visual cortex. Nature. 2005
14. Lin YJ, Koretsky AP. Manganese ion enhances T_1-weighted MRI during brain activation: an approach to direct imaging of brain function. Magn Reson Med 1997;38:378–388. [PubMed: 9339438]
15. Pautler RG, Koretsky AP. Tracing odor-induced activation in the olfactory bulbs of mice using manganese-enhanced magnetic resonance imaging. Neuroimage 2002;16:441–448. [PubMed: 12030829]

•16. Lee JH, Silva AC, Merkle H, Koretsky AP. Manganese-enhanced magnetic resonance imaging of mouse brain after systemic administration of $MnCl_2$: dose-dependent and temporal evolution of T_1 contrast. Magn Reson Med 2005;53:640–648. [PubMed: 15723400] [This paper presents a thorough investigation of the influence of Mn^{2+} infusion parameters on the time course of MRI contrast changes in mice. The study is an excellent reference for those contemplating use of the Mn^{2+} labeling technique for activity mapping experiments]

•17. Yu X, Wadghiri YZ, Sanes DH, Turnbull DH. In vivo auditory brain mapping in mice with Mn-enhanced MRI. Nat Neurosci 2005;8:961–968. [PubMed: 15924136] [The authors used Mn^{2+} labeling methods to generate 100 μm isotropic resolution maps of auditory activity in mice. Visually compelling data demonstrate tone-specific uptake of the tracer in longitudinal studies and in a comparison of normal and partially deafened animals. The study is notable for demonstrating capabilities of the only molecular fMRI technique now in widespread use]

18. Watanabe T, Schachtner J, Krizan M, Boretius S, Frahm J, Michaelis T. Manganese-enhanced 3D MRI of established and disrupted synaptic activity in the developing insect brain in vivo. J Neurosci Methods 2006;158:50–55. [PubMed: 16766041]
19. Li W, Fraser SE, Meade TJ. A Calcium-Sensitive Magnetic Resonance Imaging Contrast Agent. J. Am. Chem. Soc 1999;121:1413–1414.

•20. Atanasijevic T, Shusteff M, Fam P, Jasanoff A. Calcium-sensitive MRI contrast agents based on superparamagnetic iron oxide nanoparticles and calmodulin. Proc Natl Acad Sci U S A 2006;103:14707–14712. [PubMed: 17003117] [The authors use a highly efficient SPIO-based contrast mechanism to build calcium sensors with micromolar affinity for calcium and extremely

high relaxivity. High relaxivity means that low amounts of the sensor can be used (~ 1 nM), reducing the amount of calcium buffering and simplifying the challenge of brain delivery. Additional advantages of this architecture include ease of synthesis and ”tunability,” because the sensor is actuated by protein domains]

21. Shapiro MG, Atanasijevic T, Faas H, Westmeyer GG, Jasanoff A. Dynamic imaging with MRI contrast agents: quantitative considerations. Magn Reson Imaging 2006;24:449–462. [PubMed: 16677952]
22. Muldoon LL, Sandor M, Pinkston KE, Neuwelt EA. Imaging, distribution, and toxicity of superparamagnetic iron oxide magnetic resonance nanoparticles in the rat brain and intracerebral tumor. Neurosurgery 2005;57:785–796. discussion 785−796. [PubMed: 16239893]
23. Shapiro EM, Gonzalez-Perez O, Manuel Garcia-Verdugo J, Alvarez-Buylla A, Koretsky AP. Magnetic resonance imaging of the migration of neuronal precursors generated in the adult rodent brain. Neuroimage. 2006
24. Hanaoka K, Kikuchi K, Urano Y, Narazaki M, Yokawa T, Sakamoto S, Yamaguchi K, Nagano T. Design and synthesis of a novel magnetic resonance imaging contrast agent for selective sensing of zinc ion. Chem Biol 2002;9:1027–1032. [PubMed: 12323377]
25. Que EL, Chang CJ. A smart magnetic resonance contrast agent for selective copper sensing. J Am Chem Soc 2006;128:15942–15943. [PubMed: 17165700]
••26. Zhang X, Lovejoy KS, Jasanoff A, Lippard SJ. Water-soluble porphyrins as a dual-function molecular imaging platform for MRI and fluorescence zinc sensing. Proc Natl Acad Sci U S A 2007;103:10780–10785. [PubMed: 17578918] [The contrast agent introduced in this paper constitutes a rare departure from gadolinium-based synthetic agents. A manganese porphyrin platform for ion sensing (in this case zinc) offers comparable T_1 relaxivity to Gd^{3+} agents, in addition to the critical property of membrane permeability, demonstrated by cellular uptake of the new sensor]
27. Chesler M. Regulation and modulation of pH in the brain. Physiol Rev 2003;83:1183–1221. [PubMed: 14506304]
28. Gillies RJ, Raghunand N, Garcia-Martin ML, Gatenby RA. pH imaging. A review of pH measurement methods and applications in cancers. IEEE Eng Med Biol Mag 2004;23:57–64. [PubMed: 15565800]
29. Garcia-Martin ML, Martinez GV, Raghunand N, Sherry AD, Zhang S, Gillies RJ. High resolution pH(e) imaging of rat glioma using pH-dependent relaxivity. Magn Reson Med 2006;55:309–315. [PubMed: 16402385]
30. Raghunand N, Howison C, Sherry AD, Zhang S, Gillies RJ. Renal and systemic pH imaging by contrast-enhanced MRI. Magn Reson Med 2003;49:249–257. [PubMed: 12541244]
31. Raghunand N, Zhang S, Sherry AD, Gillies RJ. In vivo magnetic resonance imaging of tissue pH using a novel pH-sensitive contrast agent, GdDOTA-4AmP. Acad Radiol 2002;9(Suppl 2):S481–483. [PubMed: 12188315]
32. Zhou J, Payen JF, Wilson DA, Traystman RJ, Van Zijl PC. Using the amide proton signals of intracellular proteins and peptides to detect pH effects in MRI. Nat Med 2003;9:1085–1090. [PubMed: 12872167]
33. Vanzetta I, Hildesheim R, Grinvald A. Compartment-resolved imaging of activity-dependent dynamics of cortical blood volume and oximetry. J Neurosci 2005;25:2233–2244. [PubMed: 15745949]
34. Ogawa S, Lee TM, Kay AR, Tank DW. Brain magnetic resonance imaging with contrast dependent on blood oxygenation. Proc Natl Acad Sci U S A 1990;87:9868–9872. [PubMed: 2124706]
35. Sun PZ, Schoening ZB, Jasanoff A. In vivo oxygen detection using exogenous hemoglobin as a contrast agent in magnetic resonance microscopy. Magn Reson Med 2003;49:609–614. [PubMed: 12652529]
•36. Golman K, in 't Zandt R, Thaning M. Real-time metabolic imaging. Proc Natl Acad Sci U S A 2006;103:11270–11275. [PubMed: 16837573] [^{13}C-labeled pyrvate was hyperpolarized and injected into rats and pigs, allowing imaging with millimeter spatial resolution. Using spectroscopic MRI techniques, the authors were able to generate simultaneous maps of pyruvate, lactate, and alanine, enabling them to determine metabolic turnover rates between the species over tens of seconds. This unusual approach to molecular imaging might eventually prove useful for fMRI]

37. Ardenkjaer-Larsen JH, Fridlund B, Gram A, Hansson G, Hansson L, Lerche MH, Servin R, Thaning M, Golman K. Increase in signal-to-noise ratio of > 10,000 times in liquid-state NMR. Proc Natl Acad Sci U S A 2003;100:10158–10163. [PubMed: 12930897]

38. McCarney ER, Armstrong BD, Lingwood MD, Han S. Hyperpolarized water as an authentic magnetic resonance imaging contrast agent. Proc Natl Acad Sci U S A 2007;104:1754–1759. [PubMed: 17264210]

39. Miyawaki A, Llopis J, Heim R, McCaffery JM, Adams JA, Ikura M, Tsien RY. Fluorescent indicators for Ca^{2+} based on green fluorescent proteins and calmodulin. Nature 1997;388:882–887. [PubMed: 9278050]

40. Miesenbock G, De Angelis DA, Rothman JE. Visualizing secretion and synaptic transmission with pH-sensitive green fluorescent proteins. Nature 1998;394:192–195. [PubMed: 9671304]

41. Gillis P, Koenig SH. Transverse relaxation of solvent protons induced by magnetized spheres: application to ferritin, erythrocytes, and magnetite. Magn Reson Med 1987;5:323–345. [PubMed: 2824967]

••42. Genove G, DeMarco U, Xu H, Goins WF, Ahrens ET. A new transgene reporter for in vivo magnetic resonance imaging. Nat Med 2005;11:450–454. [PubMed: 15778721] [This article demonstrates that viral transfection of heavy and light chain Ft causes T_2 contrast in mice. As the closest analog to a "GFP for MRI," Ft could be used in the future as a marker for gene expression, or a basis for functional imaging probes]

43. Deans AE, Wadghiri YZ, Bernas LM, Yu X, Rutt BK, Turnbull DH. Cellular MRI contrast via coexpression of transferrin receptor and ferritin. Magn Reson Med 2006;56:51–59. [PubMed: 16724301]

•44. Cohen B, Ziv K, Plaks V, Israely T, Kalchenko V, Harmelin A, Benjamin LE, Neeman M. MRI detection of transcriptional regulation of gene expression in transgenic mice. Nat Med 2007;13:498–503. [PubMed: 17351627] [This paper addresses important questions about Ft-mediated contrast: Can contrast be recognized in transgenic animals? Does contrast generalize to multiple tissues? Can contrast be produced by sparse Ft-expressing cell populations? Answers seem to be "yes," according to analysis of transgenic mice conditionally expressing heavy chain Ft in vascular endothelial cells]

•45. Gilad AA, McMahon MT, Walczak P, Winnard PT Jr. Raman V, van Laarhoven HW, Skoglund CM, Bulte JW, van Zijl PC. Artificial reporter gene providing MRI contrast based on proton exchange. Nat Biotechnol 2007;25:217–219. [PubMed: 17259977] [The authors generated chemical exchange-based contrast using a *de novo* designed lysine-rich protein (LRP). Xenografts expressing the gene could be distinguished from control tumors in implanted mice. With respect to Ft, LRP is likely to have advantages and disadvantages as a marker protein for MRI]

46. Clayton DF. The genomic action potential. Neurobiol Learn Mem 2000;74:185–216. [PubMed: 11031127]

47. Louie AY, Huber MM, Ahrens ET, Rothbacher U, Moats R, Jacobs RE, Fraser SE, Meade TJ. In vivo visualization of gene expression using magnetic resonance imaging. Nat Biotechnol 2000;18:321–325. [PubMed: 10700150]

48. Weissleder R, Moore A, Mahmood U, Bhorade R, Benveniste H, Chiocca EA, Basilion JP. In vivo magnetic resonance imaging of transgene expression. Nat Med 2000;6:351–355. [PubMed: 10700241]

49. Gilad AA, Winnard PT Jr. van Zijl PC, Bulte JW. Developing MR reporter genes: promises and pitfalls. NMR Biomed 2007;20:275–290. [PubMed: 17451181]

50. Sosnovik DE, Weissleder R. Emerging concepts in molecular MRI. Curr Opin Biotechnol 2007;18:4–10. [PubMed: 17126545]

51. Westmeyer GG, Jasanoff A. Genetically controlled MRI contrast mechanisms and their prospects in systems neuroscience research. Magn Reson Imaging. 2007

52. Liu CH, Kim YR, Ren JQ, Eichler F, Rosen BR, Liu PK. Imaging cerebral gene transcripts in live animals. J Neurosci 2007;27:713–722. [PubMed: 17234603]

53. Su W, Mishra R, Pfeuffer J, Wiesmuller KH, Ugurbil K, Engelmann J. Synthesis and cellular uptake of a MR contrast agent coupled to an antisense peptide nucleic acid--cell- penetrating peptide conjugate. Contrast Media Mol Imaging 2007;2:42–49. [PubMed: 17318918]

54. Roch A, Gossuin Y, Muller RN, Gillis P. Superparamagnetic colloid suspensions: Water magnetic relaxation and clustering. J Magn Magn Mater 2005;293:532–539.

55. Josephson L, Perez JM, Weissleder R. Magnetic Nanosensors for the Detection of Oligonucleotide Sequences. Angew Chem Int Ed Engl 2001;40:3204–3206.

56. Pautler RG, Silva AC, Koretsky AP. In vivo neuronal tract tracing using manganese-enhanced magnetic resonance imaging. Magn Reson Med 1998;40:740–748. [PubMed: 9797158]

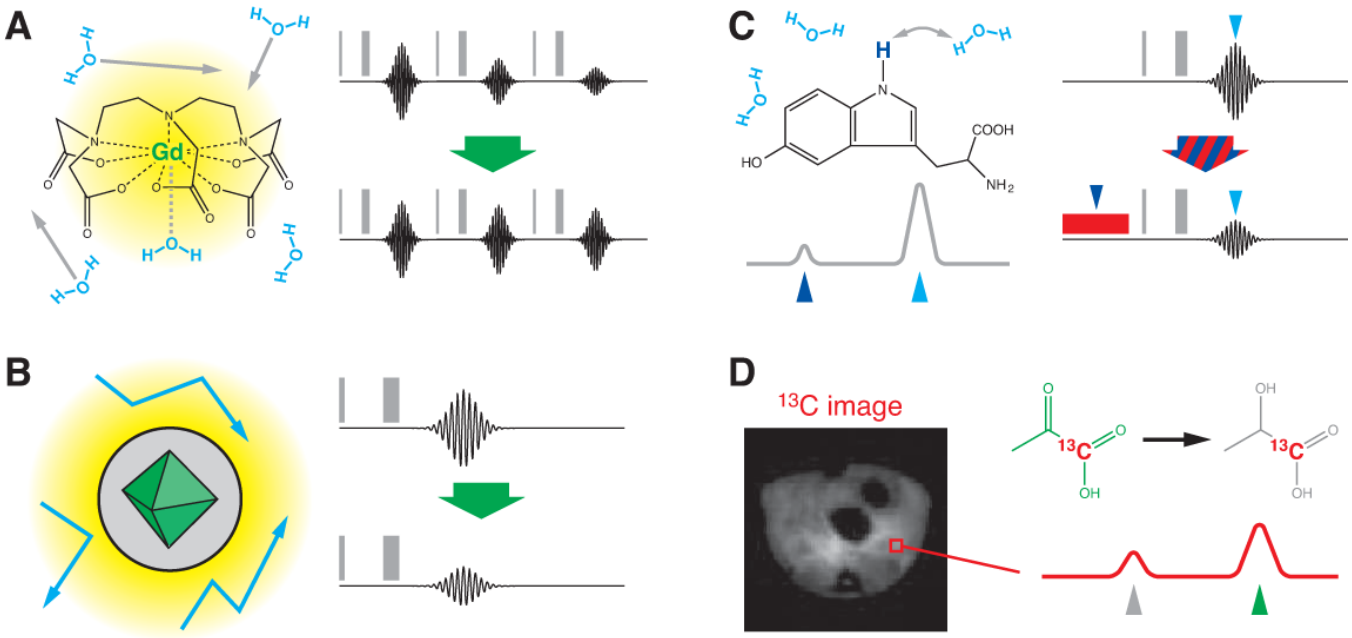

Figure 1. Contrast mechanisms in molecular MRI

Signal in MRI is proportional to the concentration of directly detected nuclei in the specimen (usually protons in water molecules), the degree to which these nuclei are polarized by the scanner's magnetic field, manipulations due to MRI acquisition schemes called pulse sequences, and the relaxation rates (T_1 and T_2) that determine how quickly nuclei in the specimen return to equilibrium after being manipulated by the pulse sequence. (A) Paramagnetic atoms promote T_1 relaxation-based contrast in conventional MRI by interacting with water molecules (left). Gadolinium atoms (green) are effective at this because of their high electron spin ($S = 7/2$); Mn^{2+} ($S = 5/2$) and a variety of other metal ions may also be used. These atoms are often incorporated into chelates (Gd^{3+}-dielthylenetriaminepentaacetic acid shown) to improve solubility and reduce toxicity. Relaxation occurs when water molecules (cyan) sample magnetic field perturbations (yellow) created by the paramagnetic atom, either through direct coordination (dotted gray line), or through space. Sensors may be constructed by making aspects of this interaction dependent on an environmental variable or molecular target. T_1-weighted imaging (right) may be performed using a variety of pulse sequences. Following one or more pulses (vertical gray bars), image data are acquired in the Fourier domain (black trace). Repetition of the pulse sequence causes progressive attenuation due to saturation of the signal, toward a steady state value that determines image intensity (top right). Addition of a T_1 contrast agent relieves this effect (bottom right) and leads to image brightening in areas where the contrast agent is concentrated. (B) Although most paramagnetic contrast agents induce both T_1 and T_2 relaxation, superparamagnetic nanoparticles including SPIOs have the highest T_2 relaxivity, and relatively low T_1 relaxivity. SPIOs typically contain a core of iron oxide 3−10 nm diameter (green), surrounded by a biocompatible organic coating with a total diameter of 10−100 nm (gray). Particles induce magnetic perturbations (yellow) that induce relaxation of water molecules diffusing in proximity (blue arrows). The particle size and shape of its field perturbation influence its relaxivity [54]—this relationship is the basis of sensors formed by making SPIO aggregation dependent on presence of a target molecule [55]. T_2 relaxation occurs during the time between each application of the pulse sequence and acquisition of the signal (black traces, right). Addition of a T_2 contrast agent causes reduction of the MRI signal (bottom right) and leads to image darkening in areas where the contrast agent is concentrated. (C) Chemical exchange saturation transfer (CEST) contrast can be produced using agents with exchangeable protons that have MRI resonance frequencies (chemical shifts)

well resolved from the frequency of water molecules [5]. The example shown is the indole nitrogen proton (indigo) of 5-hydroxytryptophan. The spectrum of chemical shifts in a solution of this agent is schematized by the gray trace at the bottom left, where resonances of the CEST agent protons and water protons are indicated by indigo and cyan arrowheads, respectively. CEST contrast is produced by modifying a typical imaging pulse sequence to include a continuous saturation pulse or pulse train (red box, bottom right) matched to the frequency of the CEST protons. The saturation pulse directly decreases MRI signal due to the CEST protons (which are usually too dilute to image), but indirectly reduces signal from water protons (cyan arrowhead) because they are in exchange with the CEST proton pool. This effect leads to local darkening of MRI signal in areas where CEST agents are concentrated; contrast may be turned on and off by changing the power or frequency associated with the saturation pulse. Sensors may be based on modulation of the exchange rate or resonance frequency of labile protons on a CEST agent. (D) Contrast agents incorporating ^{13}C, ^{19}F, or a variety of other nuclei may be imaged directly using modified MRI hardware. Images of ^{13}C agent distribution may be formed, analogous to standard proton images, but typically with much lower resolution and signal-to-noise ratio. Spectroscopic imaging techniques measure the distribution of species with different chemical shifts at each position in space (red trace). In experiments of Golman *et al.* [36], carbon resonances of $^{13}C_1$-labeled pyruvate (green) and its reduction product $^{13}C_1$-lactate (gray) could be distinguished using this approach (right). Relative amounts of the two species were indicative of local metabolic rate. Images like the one shown (left) were obtained only with the use of ^{13}C-labeled agents that had been hyperpolarized to boost MRI signal, prior to imaging [37].

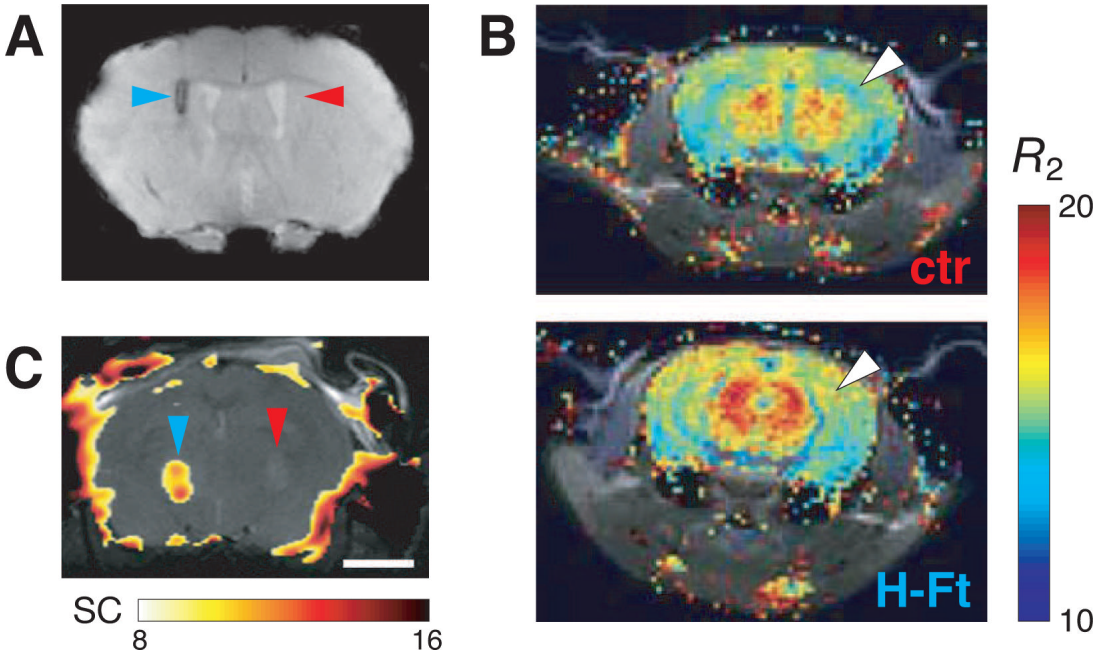

Figure 2. Genetically-encoded MRI contrast agents

(A) T_2-weighted MRI contrast observed 11 days after adenoviral transfection of ferritin heavy and light chain (H-Ft and L-Ft) genes into mouse striatum (coronal section shown). Signal darkening (cyan arrowhead) was associated with Ft expression, confirmed by immunohistochemistry. Injection with control virus harboring the *lacZ* gene (red arrowhead) did not produce MRI signal changes. Images were obtained in a 11.7 T scanner with a resolution of 0.1 × 0.1 × 0.75 mm. Adapted from ref. [42] with permission. (B) Comparison of R_2 maps ($R_2 = 1/T_2$) obtained from mice expressing H-Ft in vascular endothelial cells (bottom) with non-expressing control animals (top). Color maps show R_2 values ranging from 10–20 s^{-1}, superimposed on gray anatomical scans from the same animals at 4.7 T (234 μm in-plane resolution). Significant differences in R_2 were observed in hippocampus (white arrowhead), despite the relatively low fraction of cells expressing Ft. Adapted from ref. [44] with permission. (C) A map of CEST contrast (difference in signal between on-resonance and off-resonance saturation conditions, see Figure 1C) in mouse brains containing xenografted 9L rat glioma cells expressing LRP (left, cyan arrowhead) or GFP (right, red arrowhead). CEST signal (0.56 mm in-plane resolution at 11.7 T) is expressed as percent intensity difference with respect to baseline in the brain (color scale), overlaid on a corresponding anatomical image (gray). LRP expressing tumors showed 8.2 ± 3.2% intensity difference, *vs.* 3.5 ± 3.3% for controls. Apparent CEST contrast outside the brain is due to magnetic field inhomogeneities, which dramatically influence results from this technique. Scale bar = 2 mm. Adapted from ref. [45] with permission.

Table 1

Selected MRI contrast agents with possible utility for functional brain imaging.

Contrast Agent	Application	Advantages	Limitations
Indicators for Ca^{2+} and other metal ions			
Mn^{2+} as Ca^{2+} mimetic [14,15,56]	> 100 μm resolution T_1-weighted activity mapping and tract tracing.	Mn^{2+} labeling is performed prior to imaging; signal persists for hours.	Long labeling times required. Real time imaging not feasible.
BAPTA-based Gd^{3+} complex (Gd-DOPTA) [19]	T_1 relaxivity change (3.3−5.8 $mM^{-1}s^{-1}$) demonstrated *in vitro* (11.7 T).	Strong relaxivity change for a Gd^{3+} agent. Likely fast Ca^{2+} responses.	Not yet applied *in vivo*. High concentrations (10 −100 μM) required.
SPIOs conjugated to calmodulin (CaM) and CaM targets [20]	T_2 relaxivity change [200 to 40 $(mM\ Fe)^{-1}s^{-1}$] observed *in vitro* (4.7 T).	Low concentrations may be used. Easy synthesis with "tunable" affinity.	Not yet applied *in vivo*. Slow response kinetics and large size (50 nm).
Mn^{3+}-porphyrin zinc sensor [$(DPA\text{-}C_2)_2$-Mn-$TPPS_3$] [26]	2 to 5-fold T_1 and T_2 changes seen with 100 μM agent in cells (4.7 T).	Agent is membrane permeable. Metal-free analog is fluorescent.	Reversibility and relaxivity mechanism not yet established.
pH indicators			
Endogenous amide protons [32]	0.5 pH unit changes observed by CEST imaging in rats (4.7 T).	Endogenous contrast source suitable for human imaging.	0.2 unit pH changes relevant to brain function probably undetectable.
Phosphonated Gd^{3+} complex ($GdDOTA\text{-}4AmP^{5-}$) [31]	T_1 relaxivity change 3.5−6.8 with vascular pH drop from 8 to 6 (4.7 T).	Compatible with high resolution imaging. Calibration possible.	0.2 unit pH changes may be undetectable. Delivery route required.
Probes for metabolic activity			
Exogenous hemoglobin [35]	Signal changes of 50% observed in fly brains with O_2 0−21%.	Large T_2-relaxivity change (0−7 $mM^{-1}s^{-1}$ at 14.1 T).	Sensitivity not ideally matched to PO_2 in brain. fMRI not demonstrated.
Hyperpolarized $^{13}C_1$-pyruvate [36]	Millimeter-resolution ^{13}C image series acquired over 40 s at 1.5 T.	Multiple species tracked at once. Agents almost identical to metabolites.	Only low resolution possible. Constant supply of agent required.
Genetically-controlled contrast agents			
Ferritin (Ft) [42,44]	T_2-weighted contrast detected in transfected and transgenic mice.	Contrast detectable in sparse cell populations. No apparent toxicity.	Relaxivity of Ft relatively low. Contrast changes slow to develop.
Artificial lysine-rich protein (LRP) [45]	5% signal change observed in LRP-expressing xenografts (11.7 T).	Contrast independent of prosthetic groups; may be "switched" on and off.	Long image acquisition times usually required with CEST mechanism.
Gd^{3+}-binding substrate (EGadMe) for β-galactosidase [47]	Injected frog embryos expressing β-gal showed ~ 50% signal changes.	Low levels of β-gal detected. Widespread use of β-gal as a marker.	Exogenous agent must be delivered. Relaxivity change is irreversible.
Transferrin (Tf)-conjugated SPIOs [48]	Tumors expressing transferrin receptor distinguished from controls.	SPIO agent detectable at low levels. Receptor catalyzes agent uptake.	Exogenous agent required. Contrast slow to build up and reverse.